

UCH-FC  
MAB-BMCN  
V161  
C.1



FACULTAD DE CIENCIAS - UNIVERSIDAD DE CHILE

**ROLE OF ENDOPLASMIC RETICULUM STRESS AND THE UNFOLDED PROTEIN  
RESPONSE IN LOCOMOTION RECOVERY AFTER SPINAL CORD HEMISECTION  
IN MICE.**

Tesis entregada a la Universidad de Chile en cumplimiento parcial de los requisitos  
para optar al Título de Magíster en Ciencias Biológicas Mención Biología Celular,  
Molecular y Neurociencias

Vicente Spiro Valenzuela Paterakis

Director de Seminario de Título: Dr. Claudio Hetz Flores

Co-Director de Seminario de Título: Dr. Felipe Court Goldsmith

November, 2011

Santiago – Chile

**FACULTAD DE CIENCIAS - UNIVERSIDAD DE CHILE**

**INFORME DE APROBACIÓN - TESIS DE MAGÍSTER**

Se informa a la Escuela de Postgrado de la Facultad de Ciencias que la Tesis de  
Magíster presentada por el candidato

**Vicente Spiro Valenzuela Paterakis**

Ha sido aprobado por la comisión de Evaluación de la tesis como requisito para optar  
al grado de Magíster en Ciencias con mención en Biología Molecular Celular y  
Neurociencias, en el examen de Defensa Privada de Tesis rendido el día 7 de  
Septiembre del 2011.

**Director de Tesis**

Dr. Claudio Hetz Flores



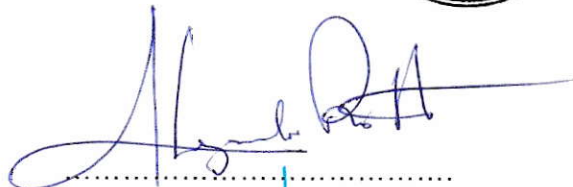
**Co-Director de Tesis**

Dr. Felipe Court Goldsmith

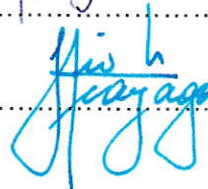


**Comisión de Evaluación de la Tesis**

Dr. Alejandro Roth Metcalfe



Dr. Julio Alcayaga Urbina





**For those who still imagine.**

## BIOGRAPHY



28 years ago and a little story began in my hometown Antofagasta, and soon I was received by Arica. My parents, Vicente and Jacqueline, my brothers Nicolas and Alexandro, they are all responsible for what I am today, and I thank you forever. The Empart, Radio El Morro, Magisterio, Liceo Domingo Santa Maria, D-4 School, Liceo A-1, friends, eternal football times, all those places witnesses of the steps that allowed me to come here. I arrived in Santiago with the curiosity to explore a career that was not sure what it was, but his name sounded interesting: Molecular Biotechnology Engineering, I went for the Bachelor Program, but already I had decided my course. In the first years of University I realized that was exactly what I was looking for: teachers with vocation, great friends, time to study but also to enjoy and most importantly, the solid foundation offered by the University of Chile to mature and become what I am. My curiosity led me through several undergraduate laboratories, including internships and research units: Palynology, Biochemistry, Plant Biology, Molecular Cell Biology and the Millennium building, all in the Faculty of Sciences. Until the seminar's title at the Laboratory of Cell Stress and Biomedicine, Faculty of Medicine and the Laboratory of Neurosciences and Glial Biology at the Catholic University, and then to extend this work in the present Master's Thesis. Family, Friends, Science, it's all that I need in this life, is what will help me on the road ahead.





**For those who still imagine.**

## ACKNOWLEDGEMENTS

I would like to acknowledge to all people who helped me to made it possible, my parents, brothers and family, my tutors, my future wife, my all-life friends, my lab mates from U. de Chile and U. Católica. Specifically thanks to Eileen Collyer, Mónica Pérez and Alejandra Catenaccio for their patience and excellent expertise.



## **ACKNOWLEDGEMENTS**

I would like to acknowledge to all people who helped me to make it possible, my parents, brothers and family, my tutors, my future wife, my all-life friends, my lab mates from U. de Chile and U. Católica. Specifically thanks to Eileen Collyer, Mónica Pérez and Alejandra Catenaccio for their patience and excellent expertise.

## FUNDING

This work was funded through projects: FONDECYT #1100176, #1070377 and #1110987, FONDAP #15010006, Millennium Nucleus #P07-048-F and #P07-011-F; and Millennium Institute P09-015-F.



# INDEX



BIOGRAPHY .....	v
ACKNOWLEDGEMENTS .....	vi
FUNDING .....	vii
INDEX .....	viii
FIGURES INDEX.....	x
ABBREVIATION INDEX .....	xi
1. ABSTRACT .....	1
2. RESUMEN.....	2
3. INTRODUCTION .....	3
3.1. The Spinal Cord.....	3
3.2. Spinal Cord Injury .....	4
3.3. Spinal Cord Injury progression.....	5
3.4. Locomotion recovery after SCI .....	9
3.6. UPR in Neurodegenerative diseases .....	11
4. HYPOTHESIS .....	13
5. GENERAL OBJECTIVE.....	13
5.1. Specific Objectives .....	13
6. MATERIALS AND METHODS .....	14
6.1. Experimental animals and surgical procedures.....	14
6.2. Western blot analysis of spinal cord extracts. ....	14
6.3. RNA Extraction and RT-PCR.....	15
6.4. Locomotor function.....	16
6.5. Histological analysis.....	16
6.6. AAV production and injection of viral particles into the spinal cord.....	17
6.7. Statistical analysis.....	18
7. RESULTS.....	19
7.1. Early activation of the UPR after spinal cord hemisection.....	19
7.2. ATF4 and XBP1 deficiency attenuates locomotor recovery after SCI.....	21

7.3. Enhanced axonal degeneration and altered cellular environment in ATF4 deficient mice after spinal cord injury.....	23
7.4. XBP1s gene transfer into the spinal cord injury site enhances locomotor recovery after SCI. ....	27
8. DISCUSSION .....	30
9. CONCLUSIONS .....	34
10. REFERENCES .....	35
11. SUPPLEMENTARY INFORMATION.....	40



## FIGURES INDEX

<b>Figure 1</b>	UPR activation after spinal cord hemisection.	<b>20</b>
<b>Figure 2</b>	Role for UPR in locomotor recovery after SCI.	<b>22</b>
<b>Figure 3</b>	Altered cellular environment in ATF4 deficient mice after SCI.	<b>24</b>
<b>Figure 4</b>	Altered inflammatory response in UPR deficient mice after SCI.	<b>26</b>
<b>Figure 5</b>	Xbp1s gene transfer with AAVs enhances locomotion recovery after SCI	<b>29</b>
<b>Figure S1</b>	ATF4 and ubiquitination levels after SCI	<b>40</b>
<b>Figure S2</b>	Altered cellular environment at 14 days post-SCI in UPR deficient mice	<b>41</b>
<b>Figure S3</b>	Xbp1s gene transfer with AAVs enhances locomotion recovery after SCI.	<b>42</b>
<b>Figure S4</b>	Analysis of UPR markers from the microarray GDS2159 in the T8 spinal cord segment up to 28 days after moderate contusion injury.	<b>43</b>

## ABBREVIATION INDEX



<b>ATF4</b>	<b>Activating transcription factor 4</b>
<b>AAV</b>	<b>Adeno-associated virus</b>
<b>BiP</b>	<b>Binding protein/Grp78</b>
<b>BMS</b>	<b>Basso Mouse Scale</b>
<b>cDNA</b>	<b>Complementary Deoxyribonucleic Acid</b>
<b>CHOP/GADD153</b>	<b>C/EBP homologous protein</b>
<b>DRP</b>	<b>DNase resistant particle</b>
<b>eIF2<math>\alpha</math></b>	<b>Eukaryotic translation initiation factor 2<math>\alpha</math></b>
<b>ER</b>	<b>Endoplasmic Reticulum</b>
<b>GFAP</b>	<b>Glial fibrillary acidic protein</b>
<b>GFP</b>	<b>Green fluorescent protein</b>
<b>HSP90</b>	<b>Heat shock protein 90</b>
<b>IRE1<math>\alpha</math></b>	<b>Inositol-requiring transmembrane kinase/endonuclease 1<math>\alpha</math></b>
<b>kDa</b>	<b>KiloDalton</b>
<b>mRNA</b>	<b>Messenger Ribonucleic Acid</b>
<b>OCT</b>	<b>Optimal Cutting Temperature</b>
<b>Pb</b>	<b>Pair Base</b>
<b>PCR</b>	<b>Polymerase Chain Reaction</b>
<b>PERK</b>	<b>PKR-like ER kinase</b>
<b>qPCR</b>	<b>Quantitative PCR</b>

**RT PCR****Reverse Transcriptase PCR**

<b>SEM</b>	<b>Standard error of the mean</b>
<b>SC</b>	<b>Spinal Cord</b>
<b>SCI</b>	<b>Spinal Cord Injury</b>
<b>Tm</b>	<b>Tunicamycin</b>
<b>UPR</b>	<b>Unfolded Protein Response</b>
<b>WT</b>	<b>Wildtype</b>
<b><i>Xbp1</i></b>	<b>Total X-Box binding protein-1 mRNA</b>
<b><i>Xbp1s</i></b>	<b>Spliced X-Box binding protein-1 mRNA</b>



## 1. ABSTRACT

Spinal cord injury (SCI) is a major cause of paralysis, and involves multiple cellular and tissue responses including demyelination, inflammation, cell death and axonal degeneration. Recent evidence suggests that endoplasmic reticulum (ER) homeostasis is perturbed in different SCI models. However, the functional contribution of this pathway to the pathology of this condition is not known. Here we demonstrate that SCI triggers a fast ER stress reaction (1-3h) involving the upregulation of key components of the unfolded protein response (UPR), a process that propagates through the spinal cord. Ablation of XBP1 or ATF4 expression, two major UPR transcription factors, leads to reduced locomotor recovery after experimental SCI. The effects of UPR inactivation were associated with a significant increase in the number of damaged axons and reduced amount of oligodendrocytes surrounding the injury zone. In addition, altered microglial activation and pro-inflammatory cytokine expression were observed in ATF4 deficient mice after SCI. Local expression of active XBP1 into the spinal cord using adeno-associated viruses enhanced locomotor recovery after SCI, and was associated with increased number of oligodendrocytes. Altogether, our results demonstrate a functional role of the UPR in SCI, offering novel therapeutic targets to treat this invalidating condition.

## 2. RESUMEN

La lesión a la médula espinal (SCI) es la mayor causa de parálisis e involucra respuestas celulares y tisulares que incluyen demielinización, muerte celular y degeneración. Evidencia reciente sugiere que existe perturbación de la homeostasis del retículo endoplasmático (ER) en diferentes modelos de SCI. Sin embargo, la contribución funcional de esta vía en la patología asociada a esta condición no ha sido esclarecida. En este trabajo se demuestra que la SCI gatilla una rápida reacción de estrés de ER (1-3h) involucrando la regulación positiva de componentes clave de la respuesta a proteínas mal plegadas (UPR), proceso que se propaga a lo largo de la médula espinal. La supresión de la expresión de las proteínas XBP1 o ATF4, dos de los principales factores de transcripción de la UPR, produce una recuperación locomotora reducida luego de una SCI. Los efectos de la inactivación de la UPR fueron asociados a una disminución significativa en el número de oligodendrocitos rodeando la zona dañada. Además, se encontraron niveles alterados de citoquinas y densidad microglial en ratones deficientes para ATF4. La expresión local de la forma activa de XBP1 en la médula espinal lesionada mediante virus adeno-asociados permitió una mejora en la recuperación locomotora post-lesión y se observó un aumento en el número de oligodendrocitos en la zona tratada. Estos resultados demuestran una función positiva de la UPR en SCI, ofreciendo nuevos blancos terapéuticos para tratar esta condición.

### **3. INTRODUCTION**

#### **3.1. The Spinal Cord**

The spinal cord (SC) is a cylindrical mass of nerve tissue that, together with the brain, constitutes the central nervous system in vertebrates. Among its functions, the SC transmits sensory and motor nerve signals to and from the brain. Additionally, the SC also functions as a generator of responses independent from the brain, from simple reflexes to more complex motor patterns, such as scratching, fast paw shake, and locomotion [1]. Structurally, the SC is organized into segments associated with spinal vertebrae, which surround and protect the entire SC. In humans, the upper portion of the spine, called cervical area has seven cervical vertebrae. The section that follows, the dorsal area, consists of twelve thoracic vertebrae. The lower back section is known as the lumbar area, where there are five lumbar vertebrae. Finally, the end section has five sacral vertebrae is called the sacral area.

The structural components of the SC are five and include (i) tracts (axons) of motor neurons that transmit signals from the brain to various body parts; (ii) tracts of sensory neurons called ganglion cells of dorsal root which carry sensory information to the SC; (iii) glial cells, which are further classified into astrocytes and oligodendrocytes. Astrocytes have varied functions, from regulating the conduction of the nerve impulse to regulate synaptic strength, while oligodendrocytes, myelinate axons increasing the velocity of action potential conduction; (iv) neurons: interneurons, located in their whole extension in the SC, help to integrate sensory information and



generate coordinated signals that control muscle contraction, and motor neurons that control muscular movement; and finally (v) the microglia, which in its activated form helps eliminate cellular debris [2].

### **3.2. Spinal Cord Injury**

Spinal Cord Injury (SCI) is an event that leads to motor and/or sensory loss, and in many cases causes paralysis for life. SCI typically is produced by a mechanical shock over the vertebrae that in turn compress the spinal cord tissue affecting the structural components mentioned. Due to mechanical force, axons in the injury site are transected and cell membranes damaged. In addition, blood-brain barrier is disrupted. Blood vessels break due to the mechanical force over them, causing severe bleeding in the inner zone of the SC, which can spread to other areas of the SC in few minutes post-injury. The severity of injury will depend on the degree of nerve fiber breakdown and the location of damage in the SC. For example, a complete section of nerve fibers in the SC is referred as spinal cord transection, which leads to total loss of voluntary movements and sensitivity; a partial damage is commonly called an incomplete SCI and can lead to a relative degree of locomotion and sensory recovery. In terms of the spatial location of the SCI and its consequences, two types of injury have been defined: paraplegia and quadriplegia. Paraplegia corresponds to the immobility and sensory loss of the lower extremities of the body. These cases occur when the injury takes place in the dorsal, lumbar or sacral area. Quadriplegia corresponds to a sensorimotor loss of

both upper and lower extremities of the body, this injury is due to SCI in the cervical area [3].

Currently in the United States there are approximately 250,000 people suffering from this physical alteration with 10,000 new cases each year. 38.5 percent of all injuries occur in car accidents, 24.5 percent, is caused by acts of violence, often involving guns and knives. The remaining cases of SCI are due to sport accidents and falls. Over 80 percent of patients with lesions of the SC are men. On the other hand, the area of greatest impact on cervical SCI includes vertebrae 4 and 6 (C4-C6) and the second highest incidence area located between the thoracic vertebra 12 (T12) and lumbar 1 (L1) [4].

During the past 50 years, major therapeutic efforts have been done to treat patients suffering SCI and improve their locomotor capabilities. In addition, researchers around the world have published numerous articles, with intentions of finding a solution to this problem. Despite this, efforts have been insufficient and there is currently no method to repair the SCI. Currently the only drug used to treat injuries to the SC are steroids such as dexamethasone or methylprednisolone applied 8 hours post-injury to reduce inflammation [5-8]. Therefore, it is essential to understand the molecular mechanisms of the SCI and the progression of this condition.

### **3.3. Spinal Cord Injury progression.**

Direct physical SCI is known as the primary injury, which occurs immediately after the traumatic event [9] causing tissue damage and therefore, changes in sensory and

locomotive capacity as mentioned above. Tissue damage during the primary injury is only the beginning of the phenomena that occur in the injured SC. The initial physical trauma to the SC causes a series of biochemical and cellular events that cause demyelination, leading to cell death of oligodendrocytes and neurons, and activation of the inflammatory response. These phenomena occur hours, days or even months after the SCI, and are known as secondary injury to the SC [9, 10]; their consequences are an increase in neurodegeneration and the formation of a glial scar, which inhibits axonal regeneration of damaged fibers.

Specifically, some of the events associated to the generation of a secondary injury are at least six. (i) The local edema and inflammation, with the consequent release of electrolytes such as potassium into the extracellular space and increased levels of sodium and chloride ions in the intracellular environment. (ii) Processes of ischemia due to hypoperfusion of blood vessels in the damaged area, slowing or even blocking action potential transmission by axons [11]. (iii) Release of free radicals such as superoxide and nitric oxide, which destroy cell membranes and triggers necrotic cell death [12-14]. Free radicals also damage the vascular integrity of neural tissue, proteins and nucleic acids [15]. (iv) Accumulation of excitatory neurotransmitters such as glutamate, which activates NMDA (N-methyl-D-aspartate) and non-NMDA receptors in neurons and glial cells. Activation of these receptors, a process known as excitotoxicity, facilitates the influx of calcium into the cell, which is an essential factor in the subsequent cell death [16]. Excess glutamate release after SCI produces hyperexcitation of neighboring cells [17], triggering a series of destructive events that culminate in cell death and release of free radicals. (v) Release of growth inhibitors which act on the damaged nerve fibers, inhibiting neuronal regeneration [14]. (vi)



Activation of a local immune response post-SCI. In the undamaged SC the blood-brain barrier prevents cells of the immune system from entering the central nervous system. However, when this barrier is permeabilized, cells of the immune system that normally circulate in the blood, particularly leukocytes, can invade the damaged tissue and trigger an inflammatory response. The inflammatory process associated with SCI is characterized by fluid accumulation and the influx of immune cells such as neutrophils, T lymphocytes, macrophages and monocytes, a process that is well characterized after the SCI [18]. The role of neuroinflammation is controversial, as both beneficial and detrimental effects have been ascribed to microglia/macrophages, lymphocytes, antibodies and cytokines [18]. Many inflammatory cytokines are similarly elevated in rodents within 24 hours of injury, including IL-1 $\beta$ , IL-2, IL-4, IL-6, TNF- $\alpha$ , and IFN- $\gamma$ . Most cytokine levels diminished by 72 hours after injury [18]. Interestingly, many immuno-stimulatory and immuno-suppressive interventions have shown positive results, which include the prevention of further tissue damage, prevention of secondary cell death and axonal degeneration, promotion of remyelination, stimulation of axonal regeneration, and facilitation of sensorimotor function recovery [19].

Another consequence of secondary injury caused by the fore-mentioned events is the activation of cellular mechanisms related to stress response or adaptation, and mechanisms of cell death when cell damage is irreversible. Several studies have suggested that programmed cell death through apoptosis plays a role in secondary injury in animal models and human tissue [20-25]. Activation of apoptosis is well described in models of SCI and has been observed in other models of nerve damage such as ischemia, several inflammatory diseases and mechanical trauma [26,

27]. Human studies show that apoptotic cells can be detected between 3 and 8 weeks after SCI [25].

At the cellular level, microglial cells are the primary mediators of the immune defense system in the CNS and are crucial for the subsequent inflammatory response. The role of microglia in the injured CNS is still controversial, as research has begun to fully explore how post-injury inflammation contributes to secondary injury and also to functional recovery. Microglia release a number of factors that modulate secondary injury and recovery after injury, including pro- and anti-inflammatory cytokines, chemokines, nitric oxide, prostaglandins, growth factors, and superoxide species [28]. Therefore, whether microglia produces positive or negative effects in locomotion after SCI is still under debate.

The environmental presence of cytokines, such as IL-1 or IFN $\gamma$  also stimulates resting astrocytes to proliferate and express proteoglycans, which are involved in the structural formation of a scar tissue within the SC, also known as the glial scar [29]. Glial cells are grouped in the area near the SCI forming the scar [30, 31], which creates a barrier that prevents an efficient axonal regeneration through this region [29]. However, the glial scar also stimulates revascularization of blood capillaries increasing the nutritional, trophic, and metabolic support of the nervous tissue [32].

Neurons and oligodendrocytes are specifically and severely affected by secondary injury after SCI [22]. In contrast, astrocytes survive and even proliferate after SCI, becoming reactive [33, 34]. Additionally, it has been recently described oligodendrogenesis [35] and proliferation of perivascular cells [36] surrounding the injury zone.

Given this confusing picture of a positive outcome by opposing treatments, we can conclude that beyond the genetic manipulation or specific therapy, the nervous system acts together and all structural components and cell-types of the SC, and their relationships are determining the fate of the particular cell. Ergo, this process of cell fate must be highly regulated.

#### **3.4. Locomotion recovery after SCI**

It has been extensively described that in many experimental models of partial injury to the SC (including contusion, compression, dorsal and unilateral hemisection), occurs recovery of locomotor capabilities [1, 37]. Locomotion recovery can be achieved by modifying the cellular environment of the injury region [38]. For example, blockade of IL-6 receptor suppresses reactive astrogliosis and decreases functional recovery after experimental SCI [39]. Additionally, locomotor recovery after SCI also has been associated with changes in synaptic plasticity, i.e. changes in the distribution of endogenous spinal networks [37].

A useful experimental model to study SCI is unilateral hemisections of the spinal cord. This type of lesion completely damages ventral and dorsal tracts on one side only, with primarily incomplete damage in the other side depending on the vertebral level injured. For example, a right unilateral hemisection at the thoracic level affects locomotion in the right hindlimb only. Following unilateral lesions in rodents, cats, and monkeys, treadmill and open field locomotion resumes within days or weeks, depending on the extent and level of the lesion (reviewed in [37]). Therefore this type of lesion



represents a useful experimental model to study factors that alters, either positively or negatively, locomotion recovery in experimental animals.

### **3.5. ER stress and the Unfolded Protein Response**

A number of pathological conditions affecting the nervous system, including SCI, can interfere with the function of a specific subcellular organelle, the endoplasmic reticulum (ER), resulting in a cellular condition termed ER stress [40]. To alleviate ER stress, an integrated signaling pathway known as the Unfolded Protein Response (UPR) is activated, which re-establishes homeostasis by decreasing the extent of protein misfolding [41, 42]. Conversely, chronic or irreversible ER stress triggers apoptosis eliminating damaged cells [43].

UPR is initiated by several stress sensors, including IRE1 $\alpha$ , which is an endoribonuclease that upon activation, initiates the splicing of the mRNA encoding the transcriptional factor X-Box-binding protein 1 (XBP1) [41, 44], converting it into a potent activator of multiple UPR-responsive genes (termed XBP1s). The product of the spliced *XBP1* mRNA (termed Xbp1s) controls the expression of survival genes involved in protein folding, secretion, and protein quality control [41, 44, 45]. Other important UPR effects are mediated by the stress sensor PERK, which phosphorylates the eukaryotic translation initiation factor 2 $\alpha$  (eIF2 $\alpha$ ), leading to a global attenuation in protein translation which decreased protein synthesis overload at the ER [46]. eIF2 $\alpha$  phosphorylation also triggers the specific translation of the transcription factor ATF4, which is essential for the upregulation of different foldases and the regulation of the

redox and metabolic status of the cell [44]. Under prolonged ER stress, ATF4 also controls the expression of pro-apoptotic components such as CHOP/GADD153 and BCL-2 family members, including BIM among others [43].

### **3.6. UPR in Neurodegenerative diseases**

Correlative studies indicate that markers of ER stress are observed in different models of SCI due to trauma (by contusion and hemisection) and ischemia [47-50]. Using a contusion model, ER stress responses were observed in the damaged zone after SCI, including XBP1 mRNA splicing, in addition to the induction of CHOP [47, 50] and BiP [49, 50]. Similarly, UPR activation was reported in spinal cord hemisection and contusion models [48]. Interestingly, signs of ER stress were also detected at some distance from the injury site [48], suggesting a spread of the pathological stress process. Similarly, damage to the spinal cord by transient ischemia correlates with increased ER stress levels [49, 51], a pathological process further enhanced by a diabetic condition [52].

In this study we describe an early upregulation of several ER stress markers in the injury zone after spinal cord hemisection, including a fast activation of XBP1 and ATF4, in addition to UPR downstream target genes including *bip*, *bim*, and *chop*. To define the possible impact of ER stress in the functional recovery after experimental SCI, we analyzed the locomotor susceptibility to SCI of ATF4 and XBP1 deficient mice. Both mouse models presented impaired locomotor recovery after SCI, associated with drastic histological changes at the level of oligodendrocyte number, microglia

activation, inflammation markers, and axonal degeneration. Treatment of mice with adeno-associated viruses (AAV) to deliver an active form of XBP1 into the spinal cord enhanced locomotor recovery. Our results indicate a functional role of the UPR in the pathogenesis of SCI, identifying an unanticipated target to treat this pathological condition affecting motor and sensory function.

#### **4. HYPOTHESIS**

Activation of the unfolded-protein response is an adaptive cellular reaction after spinal cord injury. Therefore, decreasing levels of ER stress could have a beneficial effect on locomotor recovery after spinal cord damage.

#### **5. GENERAL OBJECTIVE**

Study the role of endoplasmic reticulum stress and the UPR in locomotor recovery after spinal cord hemisection.

##### **5.1. Specific Objectives**

- To determine the rate of locomotor recovery of ATF4 and XBP1 knockout mice (*atf4<sup>-/-</sup>* and *XBP1<sup>Nes<sup>-/-</sup></sup>*, respectively).
- To assess the possible protective effects of overexpressing active XBP1 in mice by AAV-mediated intra-spinal cord injection.
- To define and compare the effects of genetic manipulation UPR in the different responses to SCI including: demyelination, axonal damage and inflammatory responses.

## **6. MATERIALS AND METHODS**

### **6.1. Experimental animals and surgical procedures.**

96 C57Bl/6 mice of 8 weeks of age, with body weight between 20 and 25 g were used in this study. ATF4 knockout mice and XBP1 conditional knockout mice were previously described [53, 54]. Mice were anesthetized with a single dose of 330 mg/Kg of 2-2-2 Tribromoethanol (Sigma) intraperitoneally. Then, the dorsal zone of the spinal cord was incised along the midline; the T12 vertebra was laminectomized to expose the spinal cord. At this level, the spinal cord was hemi-transected on the right side [55-57] using vannas microscissor (RS-5658, Roboz). Sham animals include the complete surgical procedure without hemi-transection of the spine. During recovery, mice were placed in a temperature-controlled chamber. At different days after surgery, animals were euthanized by an overdose of anesthesia. Surgical interventions and animal care follows the Institutional Review Board's Animal Care of the University of Chile (CBA # 0305 FMUCH).

### **6.2. Western blot analysis of spinal cord extracts.**

Five millimeters of spinal cord tissue containing the hemi-transected region (medial), in addition to rostral and caudal regions of the same size, were collected and homogenized in 0.1 M phosphate buffered saline (pH 7.4) containing a protease inhibitor cocktail (PIC, Roche). Half of the homogenized volume was used for protein extraction and the other half was used for RNA extraction (see below). The first volume



was re-homogenized by sonication in RIPA buffer (20 mM Tris at pH 8.0, 150 mM NaCl, 0.1% SDS, 0.5% deoxycholate, 0.5% Triton X-100) plus PIC and then samples were analyzed by SDS-PAGE. The following antibodies and dilutions were used; anti-HSP90, 1:5000 (sc-7947, H114, Santa Cruz), anti-ATF4, 1:3000 (sc-200, C-20, Santa Cruz), anti-BIM, 1:2000 (sc-8267, M-20, Santa Cruz), anti-ubiquitin 1:1000 (sc-8017, P4D1, Santa Cruz).

### **6.3. RNA Extraction and RT-PCR.**

Total RNA was prepared from spinal cord tissue previously homogenized in PBS using TRIzol (Invitrogen, Carlsbad, CA). cDNA was synthesized by iScript cDNA Synthesis (BIORAD) using random primers p(dN)6 (Roche, Basel, Switzerland). Quantitative real-time PCR was performed in an ABI PRISM7700 system (Applied Biosystems, Foster City, CA) employing SYBRgreen fluorescent reagent using standard methods [58] using the following primers:

bip forward 5'-TCATCGGACGCACTTGGAA -3'

bip reverse 5'-CAACCACCTTGAATGGCAAGA-3'

chop forward 5'-TGGAGAGCGAGGGCTTTG-3'

chop reverse 5'-GTCCCTAGCTTGGCTGACAGA-3'

actin forward 5'-CTCAGGAGGAGCAATGATCTTGAT-3'

actin reverse 5'-TACCACCATGTACCCAGGCA-3'

IL-1 $\beta$  forward 5'-CAACCAACAAGTGATATTCTCCATG-3'

IL-1 $\beta$  reverse 5'-GATCCACACTCTCCAGCTGCA-3'

IL-6 forward 5'-GAGGATACCACTCCCAACAGACC-3'

IL-6 reverse, 5'-AAGTGCATCATCGTTGTTTCATACA-3'



TNF $\alpha$  forward 5'-CATCTTCTCAAAATTCGAGTGACAA-3'

TNF $\alpha$  reverse 5'-TGGGAGTAGACAAGGTACAACCC-3'

XBP1 mRNA splicing assay was performed as previously described using PstI digestion of PCR products [59] using the following primers: mXBP1.3S (5'-AAACAGAGTAGCAGCGCAGACTGC-3') and mXBP1.2AS: (5'-GGATCTCTAAAACTAGAGGCTTGGTG-3').

#### **6.4. Locomotor function.**

Locomotor recovery was evaluated in an open-field test using the nine-point Basso Mouse Scale (BMS) [60]. The BMS analysis of hindlimb movements and coordination was performed by two independent investigators blind to the experimental condition. The final score is presented as mean +/- SEM. The eleven-point BMS subscore was used to evaluate finer aspects of locomotor capacity, which are not revealed by the BMS [60].

#### **6.5. Histological analysis.**

At 5 or 14 days after surgery, mice were perfused transcardially with 4% paraformaldehyde in 0.1 M saline phosphate buffer (PBS). A 5 mm region of the spinal cord containing the lesion site was removed and post-fixed for 3 hours in 4% paraformaldehyde. The spinal tissue was subjected to a sucrose gradient (5%, 10% and 30% sucrose in PBS), cryoprotected with OCT, and fast frozen using liquid nitrogen. The tissue was longitudinally sectioned (5  $\mu$ m thick slices) using a cryostat microtome (Leica, Nussloch, Germany). Sections were immunostained using antibodies

anti-Cd11b, 1:100 (MCA74G, Serotec), anti-NeuN, 1:300 (MAB377, Millipore Bioscience Research Reagents), anti-Olig-2, 1:200 (Q13516, Millipore Bioscience Research Reagents), and anti-GFAP, 1:1000 (N1506, Dako). Tissue sections were viewed with an Olympus IX71 microscope and images were captured using a QImaging QICAM Fast 1394 camera. Olig2-positive cells surrounding the injury zone were analyzed using a matrix of 50  $\mu\text{m}$ -separated concentric semicircles. GFAP staining intensity was calculated by creating an integrated intensity profile along the spinal cord with its center located in the injury site. Neuronal numbers were assessed by counting NeuN-positive cells in the spinal tissue, excluding the mechanically injured region. Cd11b-positive cells were determined in the region surrounding the mechanically-injured zone. All quantifications were done using ImageJ software (NIH).

#### **6.6. AAV production and injection of viral particles into the spinal cord.**

The whole Xbp-1 expression cassette was excised from pcDNA3XBP-1S as a MfeI/SphI fragment and inserted into a previral plasmid pAAVsp70 containing AAV2 inverted terminal repeats (ITRs) [61]. The vector is bicistronic and carries a GFP expression cassette that serves as a fluorescent marker for transduced cells. Recombinant AAV2.XBP1S was produced by triple transfection of 293 cells using a rep/cap plasmid and pHelper (Stratagene, La Jolla CA, USA) and purified by column affinity chromatography, as previously described [62, 63]. Viral titers were determined using a real-time TaqMan PCR assay (ABI Prism 7700; Applied Biosystems, Foster City CA, USA) with primers that were specific for the BGH poly A sequence. For animal treatment, 2  $\mu\text{l}$  of AAVs ( $10^{12}$  DRP/mL) were injected slowly over the injury site right

after performing the hemisection using a 10  $\mu$ l Hamilton syringe fitted with a 34G needle.

#### **6.7. Statistical analysis.**

Data are shown as mean  $\pm$  SEM. Statistical analyses were performed by using Student's t test or two-way repeated-measures ANOVA followed by a Bonferroni *post hoc* test for multiple comparisons. All statistical analysis were performed using GraphPad Prism 5 software.

## 7. RESULTS

### 7.1. Early activation of the UPR after spinal cord hemisection.

To monitor the occurrence of ER stress after SCI, we explored the activation of UPR components in wild type mice after spinal cord hemisection. Remarkably, a significant and progressive upregulation of XBP1 mRNA splicing was detected by RT-PCR 6 h after SCI in the injured region and was sustained for several days (Fig. 1A). Unexpectedly, we observed a significant increase in XBP1 mRNA splicing in rostral regions far from the injury zone (Fig. 1B). Coincidentally, we found a significant increase in ATF4 protein levels 6 h after SCI in the injury site, in addition to distant regions of the spinal cord (Fig. 1C). These changes were observed as early as 1 h after SCI (Fig. S1A). In agreement with these findings, we detected a sustained upregulation of classical UPR-target genes in the injury region after SCI, including *bip* and *chop* (Fig. 1D), in addition to BIM induction (Fig. 1E), a pro-apoptotic BCL-2 family member modulated by ER stress [64]. Increased accumulation of polyubiquitinated proteins was also detected after SCI, reinforcing the idea that protein folding stress occurs after SCI (Fig. S1B).



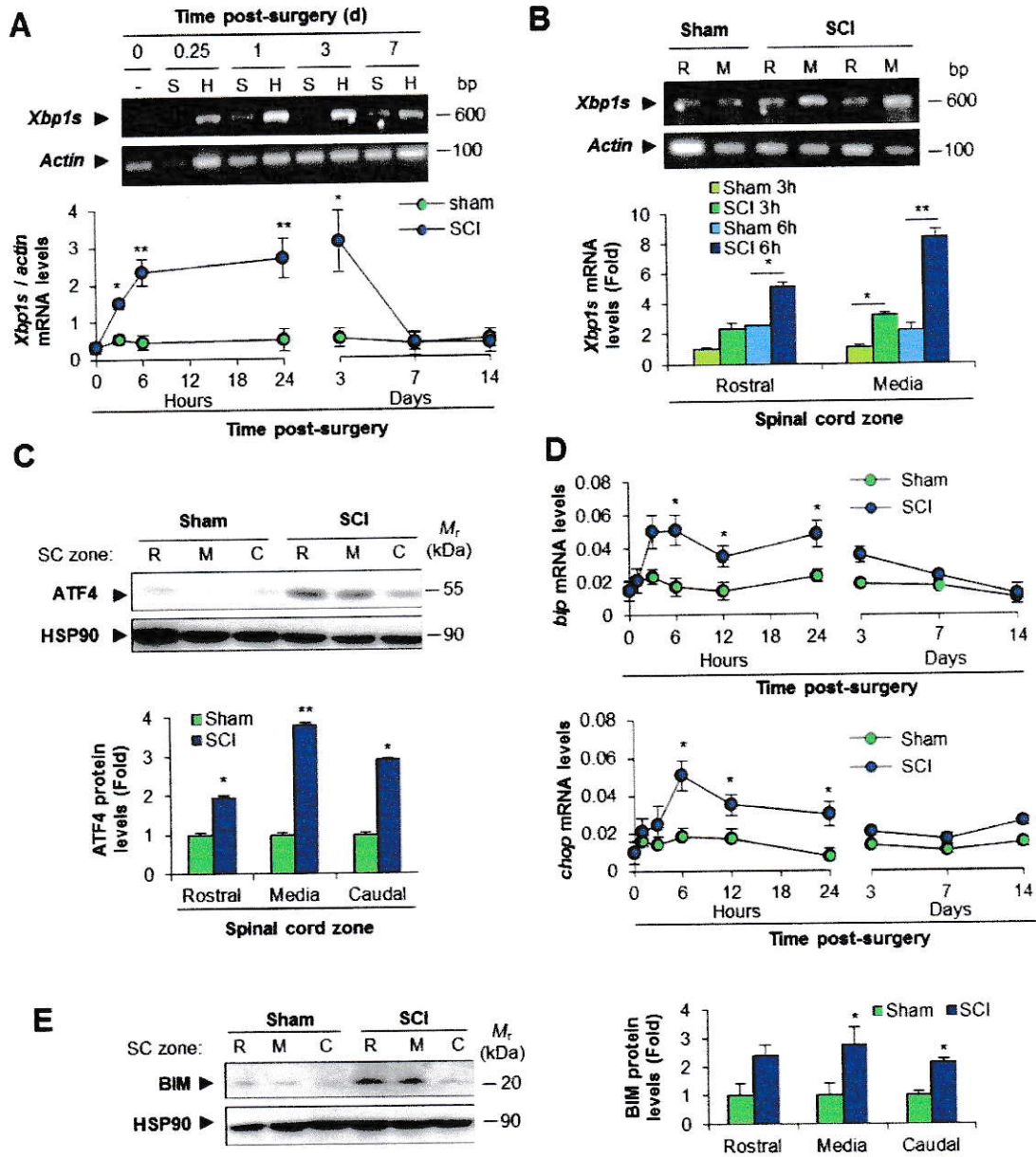


**Fig. 1. UPR activation after spinal cord hemisection.** (A) Wild type mice were spinal cord hemisected or sham operated at the T12 vertebral level. 0.25 (6 hours), 1, 3, 7 and 14 days after the surgical procedure, tissue from the operated region of the spinal cord was extracted and processed to measure spliced *Xbp1* (*Xbp1s*) mRNA levels by RT-PCR. Actin mRNA was used for normalization. (B) The same procedure was used to study *Xbp1* mRNA splicing at 3 and 6 h after SCI at the injured region (Media) and at a distance from the injury site (Rostral). *Xbp1s* levels were quantified and normalized using *actin* mRNA levels. (C) ATF4 protein levels were measured by Western blot and semi-quantified by normalizing with HSP90 protein levels. Blot and graph at 6 h after sham or hemisection from rostral (R), operated (M) and caudal (C) regions are shown. (D) *bip* and *chop* mRNA levels were quantified at the indicated times post-damage by real time PCR. (E) BIM protein levels at 6 h post SCI were measured by Western blot. Protein levels were normalized with HSP90 levels and then normalized to the sham operated condition. Mean  $\pm$  SEM. \*,  $p < 0.05$ ; \*\*,  $p < 0.005$ ; Student's *t*-test;  $n = 3$  animals per group for protein and mRNA analysis.



## 7.2. ATF4 and XBP1 deficiency attenuates locomotor recovery after SCI.

To determine a possible functional role of proximal UPR signaling components in locomotor recovery after SCI, we subjected ATF4 knockout mice (*atf4*<sup>-/-</sup>) and littermate controls to spinal cord hemisection. Analysis of locomotor activity using the Basso Mouse Scale (BMS) open field test revealed a delayed and reduced recovery of *atf4*<sup>-/-</sup> mice when compared to hemisected wild type mice (Fig. 2A left panel). A similar altered pattern was observed in the BMS subscore (Fig. 2A right panel), which discriminate differences in the fine details of locomotion that may not be apparent in the overall BMS score [60]. No differences in locomotor capacity were observed between non-injured control and *atf4*<sup>-/-</sup> mice by BMS or by monitoring rotarod performance (Fig. 2A and Fig. S2A), indicating that basal motor capacity is not compromised in *atf4*<sup>-/-</sup> mice.

Under ER stress conditions, ATF4 and XBP1 have distinct effects on ER homeostasis due to the transcriptional regulation of differential subsets of target genes [42]. To evaluate if the locomotor effects observed for ATF4 knockout mice after spinal cord hemisection are specific for this branch of the UPR or represent a more general phenomena, we evaluated the possible contribution of XBP1 to SCI. We recently generated a viable conditional knockout mouse model to delete *xbp1* in the nervous system using the Nestin promoter to express Cre (*XBP1*<sup>Nes<sup>-/-</sup></sup>), which do not present basal motor phenotypes [54]. Remarkably, *XBP1*<sup>Nes<sup>-/-</sup></sup> animals showed a marked reduction in the locomotor recovery after SCI by both the BMS score and subscore analysis (Fig. 2B), suggesting that the UPR has a broad impact on the pathological events generated after SCI.

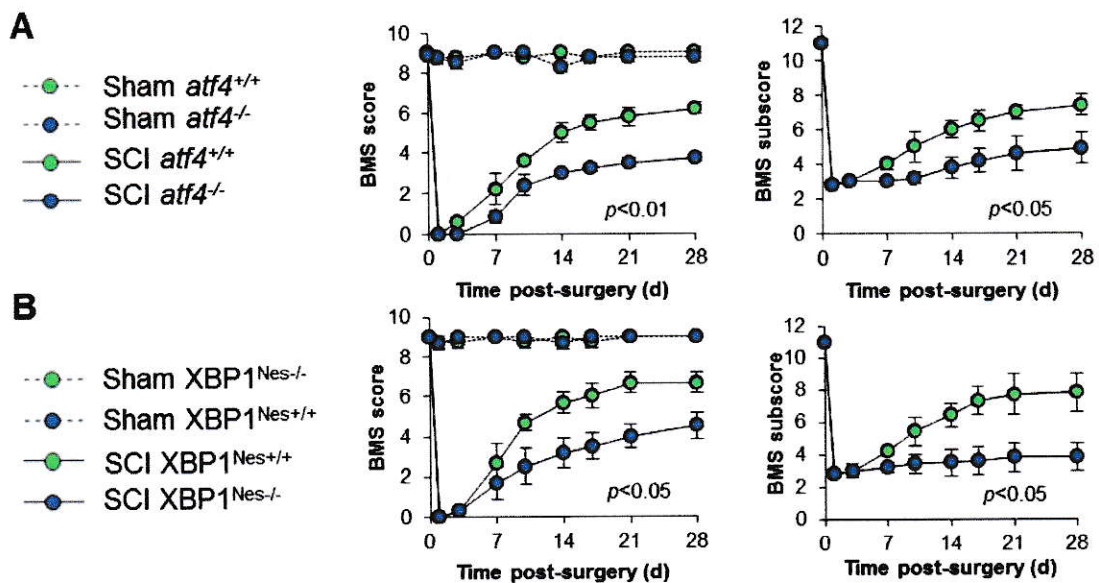


**Fig. 2. Role for UPR in locomotor recovery after SCI.** (A) *atf4*<sup>+/+</sup> and *atf4*<sup>-/-</sup> mice were hemisectioned at the T12 vertebral level. Their locomotion recovery pattern was monitored before (0d) and after spinal cord hemisection using the Basso Mouse Scale (BMS) open field test to determine their locomotor capabilities (left plot). The BMS subscore was quantified to assess locomotor recovery of finer movements (right plot). (B) The same as in A, but comparing XBP1<sup>Nes+/+</sup> and XBP1<sup>Nes-/-</sup> mice. Mean  $\pm$  SEM. Statistical differences were analyzed by a two-way repeated-measures ANOVA followed by Bonferroni's *post hoc* test; p values for SCI group comparison are indicated in the graph; n=8 animals per group.

### **7.3. Enhanced axonal degeneration and altered cellular environment in ATF4 deficient mice after spinal cord injury.**

We then evaluated the impact of targeting ATF4 on the cellular alterations classically associated to SCI. In agreement with the negative impact of ATF4 deficiency on locomotor recovery after SCI, *atf4*<sup>-/-</sup> presented less axons with normal morphology after SCI compared to control mice, measured 2 mm caudal to the injury zone in Toudine blue-stained tissue (Fig. 3A). No differences were observed in axonal density in *atf4*<sup>-/-</sup> in the contralateral, non-injured side (Fig. 3A). As a control, we performed eriochrome/cyanine staining to monitor the extent of the mechanical damage in both wild type and *atf4*<sup>-/-</sup> mice, which was virtually identical (Fig. 3B).

In addition to axonal degeneration, many different cellular processes are triggered by SCI, and involve multiple cell types. To define the impact of the UPR on the cellular environment in the injury zone of *atf4*<sup>-/-</sup> mice, we monitored glial reactions 5 days after surgery, at the beginning of the locomotor recovery phase according to the BMS score (Fig. 2). Increased accumulation of oligodendrocytes was observed in the area surrounding the injury zone of wild type mice as monitored by counting the number of olig2-positive cells by immunofluorescence (Fig. 3C and D and Fig. S2B) or by quantifying the intensity of the marker (not shown). This increase was reduced in *atf4*<sup>-/-</sup> mice (Fig. 3C).

A slight, but not statistically significant decrease in total number of neurons was observed in the injury area by NeuN staining on either control or *atf4*<sup>-/-</sup> mice after 14 days of spinal cord hemisection (Fig. S2C). We also monitored the reaction of microglia



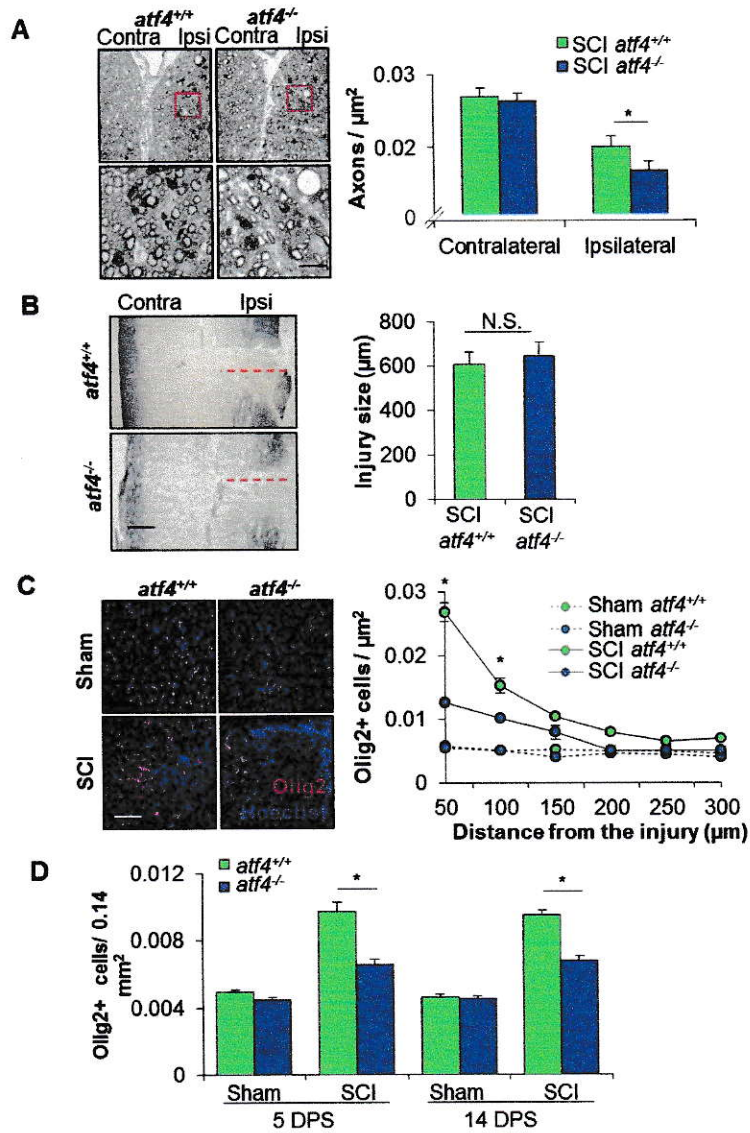


**Fig. 3. Altered cellular environment in ATF4 deficient mice after SCI.** (A) *atf4*<sup>+/+</sup> and *atf4*<sup>-/-</sup> mice were spinal cord hemisectioned or sham operated at the T12 vertebral level. 14 days after surgery, spinal cord tissue was stained with toluidin blue to study axonal integrity (left panel). Conserved axons were quantified and expressed as axonal density values (right panel). (B) Spinal cord tissue from hemisectioned *atf4*<sup>+/+</sup> and *atf4*<sup>-/-</sup> mice were longitudinally sectioned to analyze the injury size by eriochrome/cyanine myelin staining. Transversal injury length was measured from the edge of the spinal cord to the midline as shown by the red-dotted line. (C) *atf4*<sup>+/+</sup> and *atf4*<sup>-/-</sup> mice were spinal cord hemisectioned or sham operated at the T12 vertebral level. 5 days after surgery, spinal cord tissue processed for immunofluorescence for Olig2, to study oligodendrocytes (OL) and OL progenitors (red); nuclei were counterstained using Hoechst (blue). Olig2-positive particles colocalizing with Hoechst were quantified every 50  $\mu\text{m}$  starting at the injury site. (D) The same procedure as C, but total Olig2/Hoechst positive particles were quantified in a semicircular area of 300  $\mu\text{m}$  radius surrounding the injury zone at 5 and 14 days post-surgery (DPS). Mean  $\pm$  SEM. \*,  $p < 0.05$ ; \*\*,  $p < 0.005$ ; Student's *t*-test;  $n = 3$  animals per group. Scale bars, 20  $\mu\text{m}$  in A, 200  $\mu\text{m}$  in B, 100  $\mu\text{m}$  in C. Bars indicate SEM.

and astrocytes after genetically targeting ATF4. Activation of microglia was assessed using Cd11b staining. The classical microglial reaction observed after SCI was drastically reduced in *atf4*<sup>-/-</sup> mice 5 days after SCI (Fig. 4A). In sharp contrast, analysis of astrocyte distribution by GFAP immunostaining did not reveal differences between control and *atf4*<sup>-/-</sup> mice after 5 or 14 days post-SCI (Fig. 4B and Fig. S2D). General cellularity was assessed by quantifying the density of cell nucleus after Hoechst staining, which represents a measure of cellular infiltration and proliferation. This measurement was also enhanced in *atf4*<sup>-/-</sup> mice after SCI (Fig. S2E). We also monitored the levels of several pro-inflammatory cytokines that are induced upon SCI including IL-1 $\beta$ , TNF $\alpha$  and IL-6. Real time PCR analysis revealed an induction of these three cytokines in the spinal cord area surrounding the injury zone (Fig. 4C). A five-fold increase in IL-6 mRNA levels was observed in *atf4*<sup>-/-</sup> mice 6 h post hemisection (Fig. 4C). TNF $\alpha$  levels were slightly decreased in *atf4*<sup>-/-</sup>, whereas IL-1 $\beta$  were not altered (Fig. 4C). Taken together, our results indicate that ATF4 expression has a broad impact on the cellular and functional alterations observed after SCI.



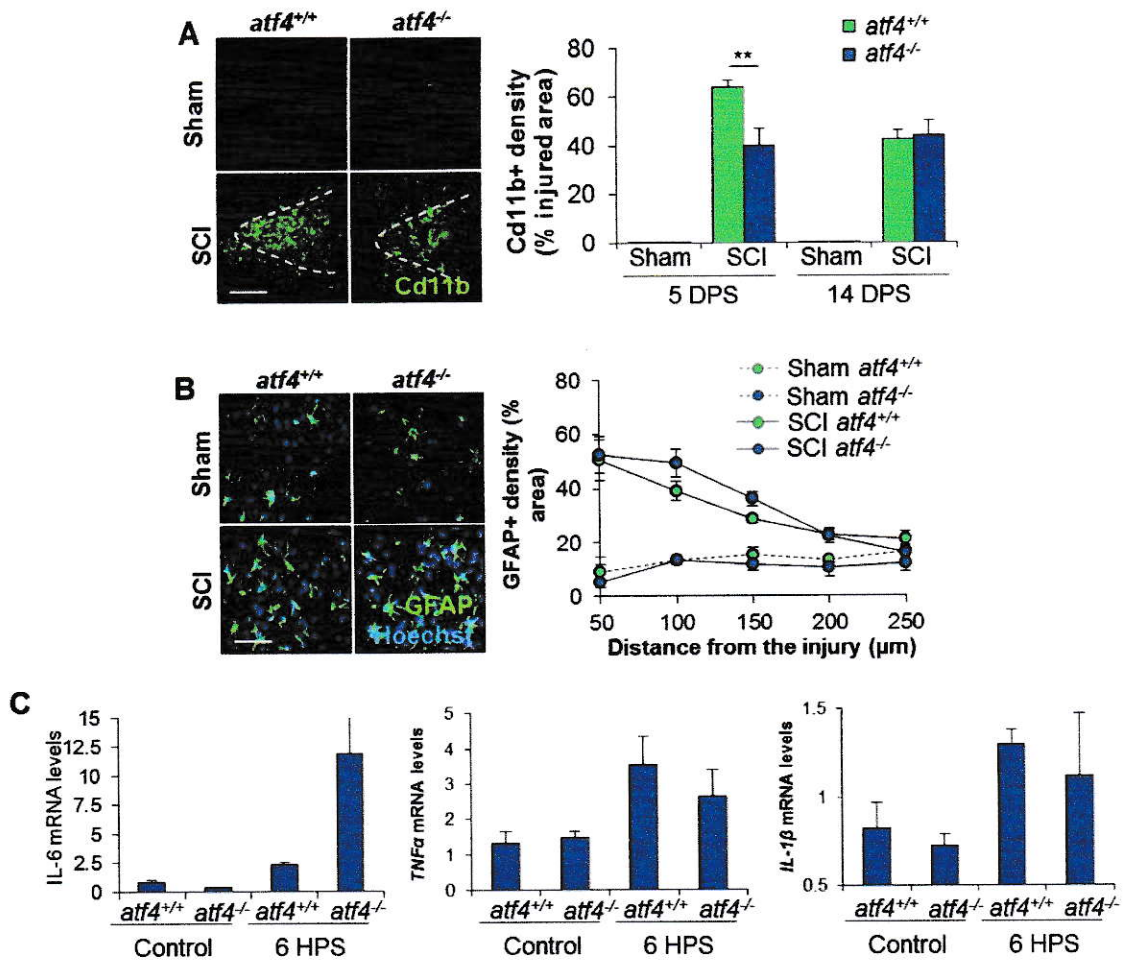


**Fig. 4. Altered inflammatory response in UPR deficient mice after SCI.** (A) *atf4*<sup>+/+</sup> and *atf4*<sup>-/-</sup> mice were spinal cord hemisectioned or sham operated at the T12 vertebral level. 5 days after surgery, spinal cord tissue was extracted and processed for immunofluorescence for the microglial marker Cd11b at the injury zone (left panel). The density for Cd11b staining was quantified at the injured zone delimited with a dotted line (right plot). (B) Activated astrocytes were studied by GFAP immunostaining. GFAP-positive label surrounding the injury zone was quantified every 50 μm from the injury (right panel). (C) Inflammatory cytokines were analyzed from injured spinal cord tissue of *atf4*<sup>+/+</sup> and *atf4*<sup>-/-</sup> mice by real time PCR 6 hours post-surgery (HPS). Mean ± SEM. \*,  $p < 0.05$ ; \*\*,  $p < 0.005$ ; Student's *t*-test;  $n = 3$  animals per group. Scale bars, 300 μm in A, 20 μm in B.

#### **7.4. XBP1s gene transfer into the spinal cord injury site enhances locomotor recovery after SCI.**

To test the possible therapeutic impact of enhancing UPR responses after SCI, we developed a gain of function approach to artificially activate the UPR by generating serotype 2 adeno-associated viruses (AAVs) to deliver the spliced form of *xbp1* into the spinal cord. GFP was expressed with a bicistronic promoter to monitor efficiency of transduction. We performed spinal cord hemisection and immediately delivered 2  $\mu$ l ( $10^{12}$  DRP/mL) of AAVs expressing empty vector or the XBP1s transgene into the injury zone. This strategy leads to a local and partial transduction of cells closely surrounding the injury site (Fig. 5A). Although the area transduced by AAVs was small, we observed a slight, but significant improvement of locomotor performance after 28 days of SCI and injection of XBP1s AAVs when compared with control virus (Fig. 5B). Furthermore, improvement of locomotor performance was evident when the BMS subscore was analyzed, which reveals finer aspects of locomotor function, observing a significant difference in the locomotor recovery of mice injected with XBP1s AAVs between 14 to 35 days after SCI (Fig. 5C and Fig. S3). The late effects of AAV-mediated delivery of XBP1s transgene are consistent with the reported delay of around 7 to 14 days for gene expression after AAVs transduction [65, 66]. Most of the cells transduced with AAVs in the spinal cord were neurons, as predicted for the serotype 2 of the viral particles (Fig. 5D). Global analysis of cellularity in the injury zone by Hoechst staining indicated a reduction of cellular density after delivering XBP1s-expressing AAVs (Fig. 5E and G). In addition, the accumulation of Olig2-positive cells was significantly increased in the injury zone of AAV-XBP1s treated mice when compared to mice injected with control viruses

(Fig. 5F and G). In summary, these results suggest that expression of active XBP1s locally into the spinal cord improved locomotor performance and augmented Olig2-positive cells after experimental SCI.

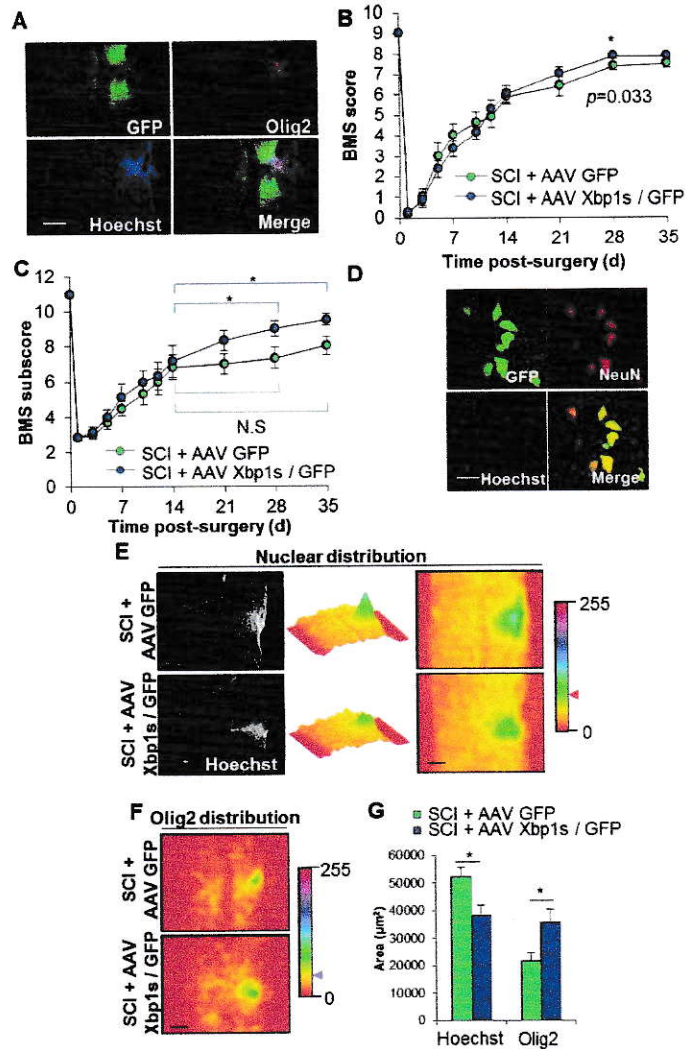


**Fig. 5. *Xbp1s* gene transfer with AAVs enhances locomotion recovery after SCI.** Wild type mice were hemisectioned at the T12 vertebral level and immediately injected into the injury site with 2  $\mu\text{l}$  ( $10^{12}$  DRP/mL) of AAV-GFP or AAV-Xbp1s/GFP. **(A)** Transduction levels were analyzed 35 days post-injection by GFP expression (green), immunolabelled with an Olig2 antibody (red) and counterstained with Hoechst (blue) in the AAV-Xbp1s/GFP injections. **(B)** Locomotion recovery pattern was monitored before (0d) and after spinal cord hemisection and viral transduction with AAV-GFP or AAV Xbp1s/GFP using the Basso Mouse Scale (BMS) open field test. **(C)** In the same groups, the BMS subscore was quantified to assess locomotor recovery of finer movements. **(D)** Neuronal-specific GFP transduction was confirmed by NeuN immunostaining (red) of spinal cord tissue injected with AAV Xbp1s/GFP (in green); nuclei were counterstained using Hoechst (blue). **(E)** Nuclear density in the injured region was analyzed by averaging Hoechst-positive nuclei intensity from 8 mice for each condition and displayed as a surface plot. The Z-axis represents average intensity in a pseudo-colored map. **(F)** Using the same approach as in E, Olig2-positive cell density was studied in AAV-GFP or AAV Xbp1s/GFP injected mice. **(G)** To quantitatively compare cellular density profiles, intensity plots of Hoechst- or Olig2-stained spinal cords from E and F, were thresholded at a fixed level (red arrowhead for Hoechst and purple arrowhead for Olig2 in the color-map shown in E), and the resulting positive area was measured and plotted. Mean  $\pm$  SEM. \*,  $p < 0.05$ ; \*\*,  $p < 0.005$ . Two-way repeated-measures ANOVA followed by Bonferroni's *post hoc* test for panels B and C;  $n = 8$  animals per group. Student's *t*-test for panel G;  $n = 8$  animals per group. Scale bars, 300  $\mu\text{m}$  in A, 20  $\mu\text{m}$  in D, 300  $\mu\text{m}$  in E and F.



## 8. DISCUSSION

Spinal cord injury is a major cause of locomotor impairment and paralysis in the world. However, the molecular events underlying the cellular and functional alterations associated with SCI are not fully understood. Identifying primary signaling events initiated by SCI is essential for future therapeutic interventions aiming to (i) restore the locomotor capacity of the affected individual or to (ii) attenuate the pathological events associated with spinal cord damage. Recent studies indicate that ER stress is an early tissue reaction after SCI in different models, including mechanical trauma and hypoxia [48-50, 67, 68]. Here we show the early activation of a range of UPR responses after SCI, including the expression of ATF4 and XBP1, major transcription factors governing this pathway, and the upregulation of downstream UPR-target genes. Remarkably, UPR activation was also observed in regions distant from the primary injury zone, suggesting the activation of a broad ER stress response in the spinal cord after damage. Interestingly, a recent report in cancer models suggested that under ER stress conditions, a transmissible signal propagates the stress response to the surrounding tissues in a pro-inflammatory related response [69], a phenomena that may also operate after SCI. We also analyzed available microarray data sets of SCI-contusion models in mice (Series GSE5296, Gene Expression Omnibus, NCBI) and observed a massive induction of ER stress responses that were sustained over time (Fig. S4).

Using genetic manipulation of the UPR we demonstrated a functional role of this stress pathway in locomotor recovery after SCI. Axonal degeneration was enhanced in



*atf4*<sup>-/-</sup> mice, correlating with impaired motor recovery after experimental SCI. Consistent with these findings, the accumulation of oligodendrocytes near the injury zone was highly reduced after deleting *atf4*. Cell-type-dependent ER stress responses have been previously observed in SCI models [49, 50]. Enhanced oligodendrogenesis was described on a contusion model of SCI [70]. Furthermore, the presence of NG2-positive cells in the injury zone correlates with improved stabilization and regeneration of dystrophic axons after SCI [71]. Remarkably, Keirstead and cols [72] reported a functional improvement of locomotion when human patients were transplanted with human embryonic cell-derived oligodendrocyte progenitor cells. We also observed differential microglial activation 5 days post-injury in *atf4*<sup>-/-</sup> mice which may contribute to the attenuated motor recovery in these mice after SCI. Interestingly, activated microglia have been suggested to attenuate oligodendrocyte precursor cell proliferation *in vitro* [73], providing a possible link between both cell type responses following SCI. Based on these findings, we speculate that the UPR may be involved in controlling oligodendrocyte-dependent protective functions in the injury site that could contribute to locomotion recovery after SCI. Our results are in agreement with a recent report indicating that ablation of the downstream pro-apoptotic ER stress factor CHOP improves motor function and oligodendrocyte viability on a contusion model of SCI [68].

ER stress is proposed to be a relevant factor in the pathogenesis of many neurodegenerative diseases involving abnormal protein folding [40]. We have previously investigated the impact of the UPR in neurodegenerative diseases. Ablation of XBP1 on a model of amyotrophic lateral sclerosis (ALS) has a contrasting effect on spinal cord from the results presented here. Despite expectations that XBP1 deficiency would enhance the pathogenesis of mutant SOD1-mediated ALS, we observed a

dramatic neuroprotection due to an enhanced clearance of mutant SOD1 aggregates by macroautophagy [74]. In contrast, XBP1 deficiency did not affect Prion misfolding or pathogenesis *in vivo* [54]. Other reports indicate that XBP1 has a protective effect on an animal model of Parkinson's disease, Alzheimer's disease, and autosomal dominant retinitis pigmentosa [40, 75]. ATF4 deficiency results in resistance to oxidative stress in models of brain ischemia [76, 77]. PERK/eIF2 $\alpha$  signaling has protective effects on axonal remyelination on models of experimental autoimmune encephalomyelitis, possibly due to the control of oligodendrocyte viability and function [78, 79]. Together with the current study, these reports suggest an intriguing scenario where the UPR may have distinct consequence depending on the nature of the pathological stimuli.

A variety of mechanisms underlying modifications of ER homeostasis may take place in specific disease contexts, and could include inhibition of ER-associated degradation, altered vesicular trafficking, altered protein folding networks among others [40]. In addition, alterations in lipid, cholesterol or calcium metabolism may also affect ER function in many diseases affecting the nervous system. Interestingly, the physiological role of the UPR has been mostly attributed to the maintenance of an efficient rate of protein synthesis and secretion in specialized secretory cells such as B lymphocytes, pancreatic beta cells, salivary glands and others [80]. Neuronal populations with higher secretory requirements might display increased sensitivity to genetic and environmental factors that disrupt ER function. In this context, oligodendrocytes and neuropeptide-secretory neurons are of particular relevance for future studies to uncover the mechanisms underlying the impact of the UPR in SCI. In fact, correlative studies suggest that the protection of valproate [67, 75] or sodium 4-phenylbutyrate [51] against SCI models can be associated with attenuated levels of ER

stress markers. The improvement obtained in locomotor function in our SCI model after XBP1s gene transfer using AAVs suggests that locomotor improvements can be achieved with treatments of days after damage (considering the delay of >1 week for gene expression after AAV gene transfer), which hold great promises as an effective therapeutic strategy to treat this invalidating condition. The use of small molecules or gene therapy strategies to attenuate ER stress or artificially engage UPR responses may have beneficial impact to attenuate tissue damage and enhance locomotor recovery in conditions affecting the function of the spinal cord.

## 9. CONCLUSIONS

We have demonstrated a functional role of the UPR in the events associated to SCI. We confirmed that SCI triggers an early activation of the UPR and plays a fundamental role in the locomotor recovery after spinal cord hemisection. We suggest that the role of the UPR in the partial locomotion recovery post-SCI is related to improvement in cellular environment surrounding the injury, more specifically by decreasing the cellular density around the injury region, as well as by maintaining an oligodendrocyte population or oligodendrocyte precursors in the damaged damage. We do not discard the possibility that the UPR may be also affecting other events involved in locomotion recovery as apoptosis or regeneration. We have shown that UPR manipulation by gene therapy is a possible strategy to improve locomotor capabilities after SCI. Despite obtaining only a local transduction after AAV injection, significant locomotor improvement of fine parameters was achieved. The next step will be to improve the efficiency of transduction, both spatially and temporally. It is important to mention that more than 40 clinical trials has been performed in humans using AAVs, and many of them in the nervous system, with proven safety issues as a therapeutic tool.

With the results presented in this thesis, it is conceivable that this methodology can be also applied to evaluate the role of the UPR in other neurodegenerative diseases, not only analyzing neurons, but the surrounding cellular environment, which can be critical for neuronal survival.



## 10. REFERENCES

1. Rossignol, S. and A. Frigon, *Recovery of locomotion after spinal cord injury: some facts and mechanisms*. Annu Rev Neurosci, 2011. **34**: p. 413-40.
2. Caspary, T. and K.V. Anderson, *Patterning cell types in the dorsal spinal cord: what the mouse mutants say*. Nat Rev Neurosci, 2003. **4**(4): p. 289-97.
3. Thuret, S., L.D.F. Moon, and F.H. Gage, *Therapeutic interventions after spinal cord injury*. Nature Rev. Neurosci., 2006. **7**: p. 628-643.
4. *Spinal cord injury. Facts and figures at a glance*. J Spinal Cord Med, 2005. **28**(4): p. 379-80.
5. Bracken, M.B., et al., *Efficacy of methylprednisolone in acute spinal cord injury*. JAMA, 1984. **251**(1): p. 45-52.
6. Behrmann, D.L., J.C. Bresnahan, and M.S. Beattie, *Modeling of acute spinal cord injury in the rat: neuroprotection and enhanced recovery with methylprednisolone, U-74006F and YM-14673*. Exp Neurol, 1994. **126**(1): p. 61-75.
7. National Institute of Neurological Disorders and Stroke (U.S.). and National Institute of Health (U.S.), *Proceedings of an NIH Workshop on Spinal Cord Injury : emerging concepts, September 30 - October 1, 1996*. NIH publication 1997, Bethesda, Md.: National Institutes of Health. 62 p.
8. Nesathurai, S., *Steroids and spinal cord injury: revisiting the NASCIS 2 and NASCIS 3 trials*. J Trauma, 1998. **45**(6): p. 1088-93.
9. Tator, C.H. and M.G. Fehlings, *Review of the secondary injury theory of acute spinal cord trauma with emphasis on vascular mechanisms*. J Neurosurg, 1991. **75**(1): p. 15-26.
10. Lu, J., K.W. Ashwell, and P. Waite, *Advances in secondary spinal cord injury: role of apoptosis*. Spine (Phila Pa 1976), 2000. **25**(14): p. 1859-66.
11. Martin, L.J., et al., *Neurodegeneration in excitotoxicity, global cerebral ischemia, and target deprivation: A perspective on the contributions of apoptosis and necrosis*. Brain Res Bull, 1998. **46**(4): p. 281-309.
12. Sandler, A.N. and C.H. Tator, *Review of the effect of spinal cord trauma on the vessels and blood flow in the spinal cord*. J Neurosurg, 1976. **45**(6): p. 638-46.
13. Amar, A.P. and M.L. Levy, *Pathogenesis and pharmacological strategies for mitigating secondary damage in acute spinal cord injury*. Neurosurgery, 1999. **44**(5): p. 1027-39; discussion 1039-40.
14. Selzer, M.E., *Promotion of axonal regeneration in the injured CNS*. Lancet Neurol, 2003. **2**(3): p. 157-66.
15. Bregman, B.S., et al., *Neurotrophic factors increase axonal growth after spinal cord injury and transplantation in the adult rat*. Exp Neurol, 1997. **148**(2): p. 475-94.
16. Ankarcrona, M., et al., *Glutamate-induced neuronal death: a succession of necrosis or apoptosis depending on mitochondrial function*. Neuron, 1995. **15**(4): p. 961-73.



17. McDonald, J.W. and C. Sadowsky, *Spinal-cord injury*. Lancet, 2002. **359**(9304): p. 417-25.
18. Donnelly, D.J. and P.G. Popovich, *Inflammation and its role in neuroprotection, axonal regeneration and functional recovery after spinal cord injury*. Exp Neurol, 2008. **209**(2): p. 378-88.
19. Chan, C.C., *Inflammation: beneficial or detrimental after spinal cord injury?* Recent Pat CNS Drug Discov, 2008. **3**(3): p. 189-99.
20. Kato, K., et al., *Induction and its spread of apoptosis in rat spinal cord after mechanical trauma*. Neurosci Lett, 1996. **216**(1): p. 9-12.
21. Li, G.L., et al., *Apoptosis and expression of Bcl-2 after compression trauma to rat spinal cord*. J Neuropathol Exp Neurol, 1996. **55**(3): p. 280-9.
22. Crowe, M.J., et al., *Apoptosis and delayed degeneration after spinal cord injury in rats and monkeys*. Nat Med, 1997. **3**(1): p. 73-6.
23. Liu, X.Z., et al., *Neuronal and glial apoptosis after traumatic spinal cord injury*. J Neurosci, 1997. **17**(14): p. 5395-406.
24. Shuman, S.L., J.C. Bresnahan, and M.S. Beattie, *Apoptosis of microglia and oligodendrocytes after spinal cord contusion in rats*. J Neurosci Res, 1997. **50**(5): p. 798-808.
25. Emery, E., et al., *Apoptosis after traumatic human spinal cord injury*. J Neurosurg, 1998. **89**(6): p. 911-20.
26. Namura, S., et al., *Activation and cleavage of caspase-3 in apoptosis induced by experimental cerebral ischemia*. J Neurosci, 1998. **18**(10): p. 3659-68.
27. Springer, J.E., R.D. Azbill, and P.E. Knapp, *Activation of the caspase-3 apoptotic cascade in traumatic spinal cord injury*. Nat Med, 1999. **5**(8): p. 943-6.
28. Loane, D.J. and K.R. Byrnes, *Role of microglia in neurotrauma*. Neurotherapeutics : the journal of the American Society for Experimental NeuroTherapeutics, 2010. **7**(4): p. 366-77.
29. Silver, J. and J.H. Miller, *Regeneration beyond the glial scar*. Nat Rev Neurosci, 2004. **5**(2): p. 146-56.
30. Windle, W.F. and W.W. Chambers, *Regeneration in the spinal cord of the cat and dog*. J Comp Neurol, 1950. **93**(2): p. 241-57.
31. Jones, L.L., D. Sajed, and M.H. Tuszynski, *Axonal regeneration through regions of chondroitin sulfate proteoglycan deposition after spinal cord injury: a balance of permissiveness and inhibition*. J Neurosci, 2003. **23**(28): p. 9276-88.
32. Stichel, C.C. and H.W. Muller, *The CNS lesion scar: new vistas on an old regeneration barrier*. Cell Tissue Res, 1998. **294**(1): p. 1-9.
33. Baldwin, S.A., et al., *Alterations in temporal/spatial distribution of GFAP- and vimentin-positive astrocytes after spinal cord contusion with the New York University spinal cord injury device*. J Neurotrauma, 1998. **15**(12): p. 1015-26.
34. Eng, L.F., R.S. Ghirnikar, and Y.L. Lee, *Glial fibrillary acidic protein: GFAP-thirty-one years (1969-2000)*. Neurochem Res, 2000. **25**(9-10): p. 1439-51.
35. Tripathi, R. and D.M.M.C. Tigue, *Prominent Oligodendrocyte Genesis Along the Border of Spinal Contusion Lesions*. Glia, 2007. **711**(January): p. 698-711.
36. Goritz, C., et al., *A Pericyte Origin of Spinal Cord Scar Tissue*. Science, 2011. **333**(6039): p. 238-242.
37. Rossignol, S., et al., *Re-expression of locomotor function after partial spinal cord injury*. Physiology (Bethesda), 2009. **24**: p. 127-39.

38. Brambilla, R., et al., *Inhibition of astroglial nuclear factor kappaB reduces inflammation and improves functional recovery after spinal cord injury*. J Exp Med, 2005. **202**(1): p. 145-56.
39. Okada, S., et al., *Blockade of interleukin-6 receptor suppresses reactive astrogliosis and ameliorates functional recovery in experimental spinal cord injury*. J Neurosci Res, 2004. **76**(2): p. 265-76.
40. Matus, S., L.H. Glimcher, and C. Hetz, *Protein folding stress in neurodegenerative diseases: a glimpse into the ER*. Current opinion in cell biology, 2011. **23**(2): p. 239-252.
41. Ron, D. and P. Walter, *Signal integration in the endoplasmic reticulum unfolded protein response*. Nat Rev Mol Cell Biol, 2007. **8**(7): p. 519-529.
42. Hetz, C. and L.H. Glimcher, *Fine-Tuning of the Unfolded Protein Response: Assembling the IRE1a Interactome*. Molecular Cell, 2009. **34**: p. 1-11.
43. Woehlbier, U. and C. Hetz, *Modulating stress responses by the UPRosome: A matter of life and death*. Trends Biochem Sci, 2011. **36**(6): p. 329-37.
44. Schroder, M. and R.J. Kaufman, *The mammalian unfolded protein response*. Annu Rev Biochem, 2005. **74**: p. 739-89.
45. Hetz, C.A., *ER stress signaling and the BCL-2 family of proteins: from adaptation to irreversible cellular damage*. Antioxid Redox Signal, 2007. **9**(12): p. 2345-55.
46. Harding, H.P., Y. Zhang, and D. Ron, *Protein translation and folding are coupled by an endoplasmic-reticulum-resident kinase*. Nature, 1999. **397**(6716): p. 271-4.
47. Penas, C., et al., *Spinal cord injury induces endoplasmic reticulum stress with different cell-type dependent response*. Society, 2007: p. 1242-1255.
48. Aufenberg, C., et al., *Spinal cord trauma activates processing of xbp1 mRNA indicative of endoplasmic reticulum dysfunction*. Journal of neurotrauma, 2005. **22**(9): p. 1018-24.
49. Yamauchi, T., et al., *Impact of the endoplasmic reticulum stress response in spinal cord after transient ischemia*. Brain Res, 2007. **1169**: p. 24-33.
50. Penas, C., et al., *Spinal cord injury induces endoplasmic reticulum stress with different cell-type dependent response*. J Neurochem, 2007. **102**(4): p. 1242-55.
51. Mizukami, T., et al., *Sodium 4-phenylbutyrate protects against spinal cord ischemia by inhibition of endoplasmic reticulum stress*. Journal of vascular surgery : official publication, the Society for Vascular Surgery [and] International Society for Cardiovascular Surgery, North American Chapter, 2010. **52**(6): p. 1580-6.
52. Wan, S., et al., *Stronger expression of CHOP and caspase 12 in diabetic spinal cord injury rats*. 2009. **000**: p. 1-7.
53. Tanaka, T., et al., *Targeted disruption of ATF4 discloses its essential role in the formation of eye lens fibres*. Genes to Cells, 1998: p. 801-810.
54. Hetz, C., et al., *Unfolded protein response transcription factor XBP-1 does not influence prion replication or pathogenesis*. Proc Natl Acad Sci U S A, 2008. **105**(2): p. 757-62.
55. Kalderon, N. and Z. Fuks, *Severed corticospinal axons recover electrophysiologic control of muscle activity after x-ray therapy in lesioned adult spinal cord*. Proc Natl Acad Sci U S A, 1996. **93**(20): p. 11185-90.



56. Fan, M., et al., *Analysis of gene expression following sciatic nerve crush and spinal cord hemisection in the mouse by microarray expression profiling*. Cell Mol Neurobiol, 2001. **21**(5): p. 497-508.
57. Boido, M., et al., *Embryonic and adult stem cells promote raphespinal axon outgrowth and improve functional outcome following spinal hemisection in mice*. Eur J Neurosci, 2009. **30**(5): p. 833-46.
58. Lee, A.H., *XBP-1 is required for biogenesis of cellular secretory machinery of exocrine glands*. EMBO J., 2005. **24**: p. 4368-4380.
59. Calton, M., et al., *IRE1 couples endoplasmic reticulum load to secretory capacity by processing the XBP-1 mRNA*. Nature, 2002. **415**(6867): p. 92-6.
60. Basso, D.M., et al., *Basso mouse scale for locomotion detects differences in recovery after spinal cord injury in five common mouse strains*. J. Neurotrauma, 2006. **23**: p. 635-659.
61. Ziegler, R.J., et al., *AAV2 vector harboring a liver-restricted promoter facilitates sustained expression of therapeutic levels of alpha-galactosidase A and the induction of immune tolerance in Fabry mice*. Mol Ther, 2004. **9**(2): p. 231-40.
62. O'Riordan, C.R., et al., *Scaleable chromatographic purification process for recombinant adeno-associated virus (rAAV)*. J Gene Med, 2000. **2**(6): p. 444-54.
63. Smith, R.H., J.R. Levy, and R.M. Kotin, *A simplified baculovirus-AAV expression vector system coupled with one-step affinity purification yields high-titer rAAV stocks from insect cells*. Mol Ther, 2009. **17**(11): p. 1888-96.
64. Puthalakath, H., et al., *ER stress triggers apoptosis by activating BH3-only protein Bim*. Cell, 2007. **129**: p. 1337-1349.
65. Davidson, B.L., et al., *Recombinant adeno-associated virus type 2, 4, and 5 vectors: transduction of variant cell types and regions in the mammalian central nervous system*. Proc Natl Acad Sci U S A, 2000. **97**(7): p. 3428-32.
66. Zincarelli, C., et al., *Analysis of AAV serotypes 1-9 mediated gene expression and tropism in mice after systemic injection*. Mol Ther, 2008. **16**(6): p. 1073-80.
67. Penas, C., et al., *Valproate reduces CHOP levels and preserves oligodendrocytes and axons after spinal cord injury*. Neuroscience, 2011: p. 1-12.
68. Ohri, S.S., et al., *Attenuating the endoplasmic reticulum stress response improves functional recovery after spinal cord injury*. Glia, 2011.
69. Mahadevan, N.R., et al., *Transmission of endoplasmic reticulum stress and pro-inflammation from tumor cells to myeloid cells*. Proceedings of the National Academy of Sciences of the United States of America, 2011: p. 1-6.
70. Tripathi, R. and D.M. McTigue, *Prominent oligodendrocyte genesis along the border of spinal contusion lesions*. Glia, 2007. **55**(7): p. 698-711.
71. Busch, S.A., et al., *Adult NG2+ cells are permissive to neurite outgrowth and stabilize sensory axons during macrophage-induced axonal dieback after spinal cord injury*. J Neurosci, 2010. **30**(1): p. 255-65.
72. Keirstead, H.S., et al., *Human embryonic stem cell-derived oligodendrocyte progenitor cell transplants remyelinate and restore locomotion after spinal cord injury*. J Neurosci, 2005. **25**(19): p. 4694-705.
73. Taylor, D.L., et al., *Attenuation of proliferation in oligodendrocyte precursor cells by activated microglia*. J Neurosci Res, 2010. **88**(8): p. 1632-44.
74. Hetz, C., et al., *XBP-1 deficiency in the nervous system protects against amyotrophic lateral sclerosis by increasing autophagy*. Genes Dev, 2009. **23**(19): p. 2294-306.

75. Ryoo, H.D., et al., *Unfolded protein response in a Drosophila model for retinal degeneration*. *Embo J*, 2007. **26**(1): p. 242-52.
76. Lange, P.S., et al., *ATF4 is an oxidative stress-inducible, prodeath transcription factor in neurons in vitro and in vivo*. *J Exp Med*, 2008. **205**: p. 1227-42.
77. Galehdar, Z., et al., *Neuronal apoptosis induced by endoplasmic reticulum stress is regulated by ATF4-CHOP-mediated induction of the Bcl-2 homology 3-only member PUMA*. *J Neurosci*, 2010. **30**(50): p. 16938-48.
78. Lin, W., et al., *The integrated stress response prevents demyelination by protecting oligodendrocytes against immune-mediated damage*. *Cell*, 2007. **117**(2).
79. Lin, W., et al., *Endoplasmic reticulum stress modulates the response of myelinating oligodendrocytes to the immune cytokine interferon- $\gamma$* . *Cell*, 2005. **169**(4): p. 603-612.
80. Hetz C, M.F., Rodriguez D, and Glimcher LH., *The Unfolded Protein Response: Integrating stress signals through the stress sensor IRE1*. *Physiological Reviews.*, 2011. **In Press**.

## 11. SUPPLEMENTARY INFORMATION

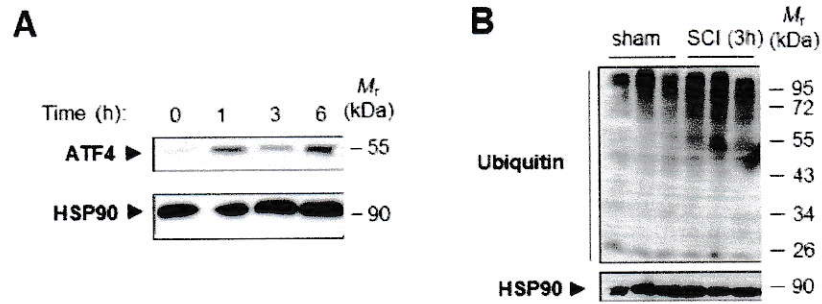


**Fig. S1. (A)** Wild type mice were spinal cord hemisected at the T12 vertebral level. 1, 3 and 6 hours after surgery, spinal cord tissue from the operated region was extracted and processed. ATF4 protein levels were analyzed by Western blot and semi-quantified by normalizing to HSP90 protein levels. Blot and graph at 1, 3 and 6 hours after spinal cord hemisection from the operated zone is shown. **(B)** Protein ubiquitination was studied by Western blot in tissue samples from spinal cord hemisected or sham operated wild type mice at the T12 vertebral level.



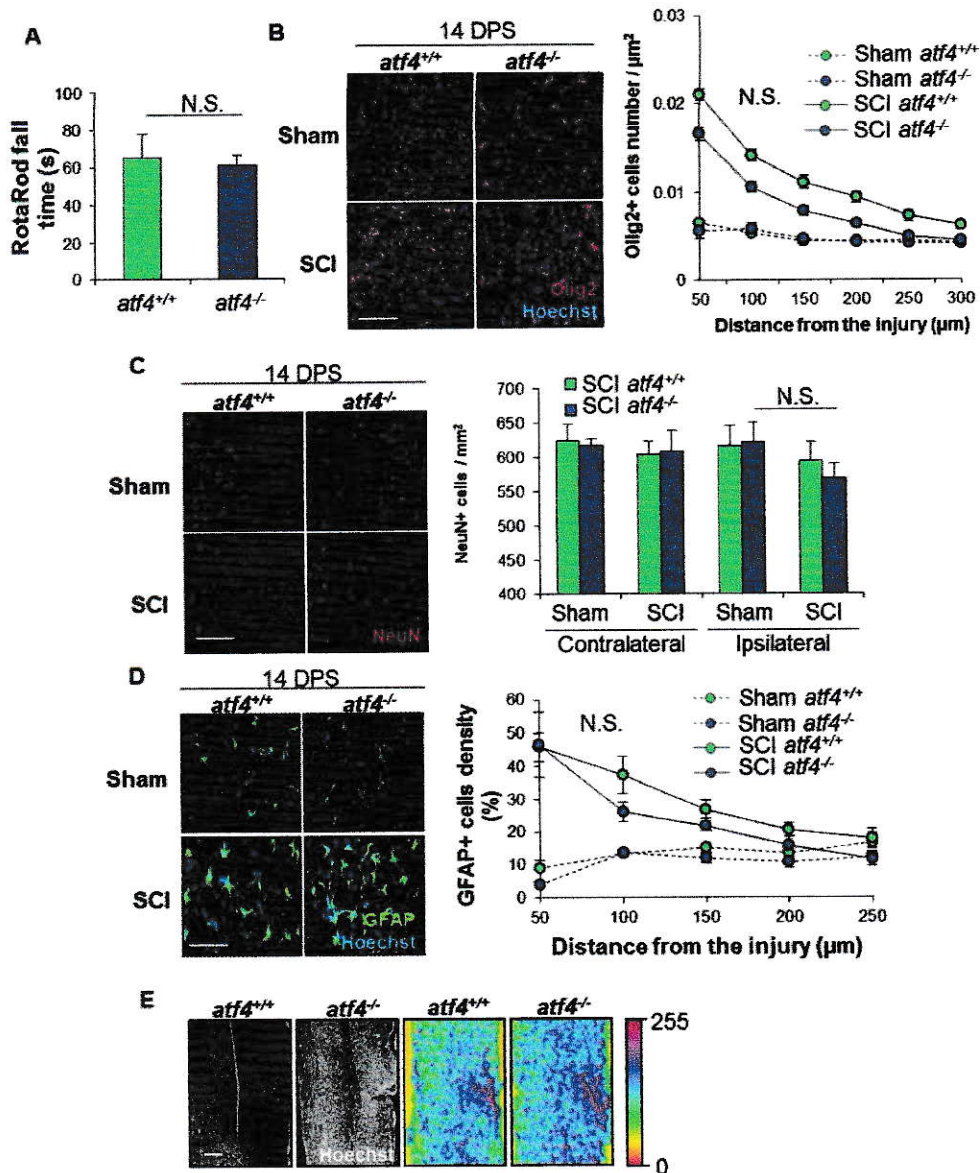


**Fig. S2. Altered cellular environment at 14 days post-SCI in UPR deficient mice.** (A) Non-injured *attf4*<sup>+/+</sup> and *attf4*<sup>-/-</sup> mice were trained and scored by the RotaRod test (ramp mode). (B) *attf4*<sup>+/+</sup> and *attf4*<sup>-/-</sup> mice were spinal cord hemisected or sham operated at the T12 vertebral level. 14 days after surgery, spinal cord tissue processed for immunofluorescence, to study oligodendrocytes (OL) and OL progenitors (red); nuclei were counterstained using Hoechst (blue). Olig2-positive particles colocalizing with Hoechst were quantified every 50 μm starting at the injury site. (C) Spinal cord neurons were analyzed by immunofluorescence using an antibody against NeuN. Neuronal density was analyzed in *attf4*<sup>+/+</sup> and *attf4*<sup>-/-</sup> mice 14 days after SCI in both contralateral and ipsilateral sides. (D) *attf4*<sup>+/+</sup> and *attf4*<sup>-/-</sup> mice were spinal cord hemisected or sham operated at the T12 vertebral level. 14 days after surgery, spinal cord tissue processed for immunofluorescence using an antibody against GFAP to study astrocytes (green); nuclei were counterstained using Hoechst (blue). GFAP-positive cells were quantified every 50 μm starting at the injury site (right panel). (E) Nuclear density in the injured region was analyzed by averaging Hoechst-positive nuclei intensity from 3 mice for each condition and displayed as a surface plot. The Z-axis represents average intensity in a pseudo-colored map. Mean +/- SEM. \*, *p*<0.05; \*\*, *p*<0.005; Student's *t*-test; n=3 animals per group for immunofluorescence analysis; n=10 for the RotaRod test. Scale bars, 100 μm in A, 200 μm in B, 20 μm in C, 300 μm in D.

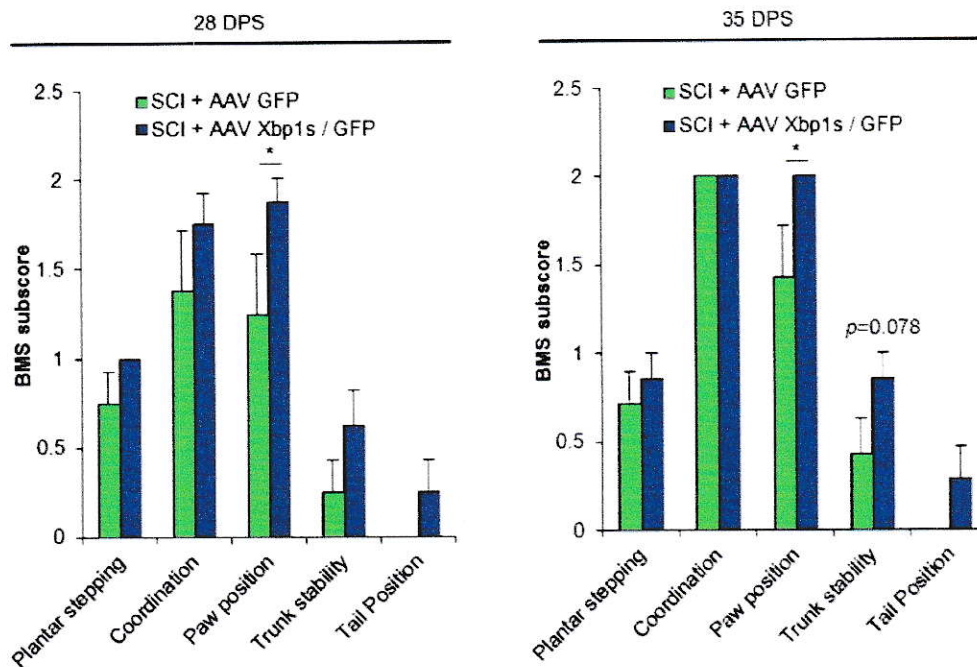
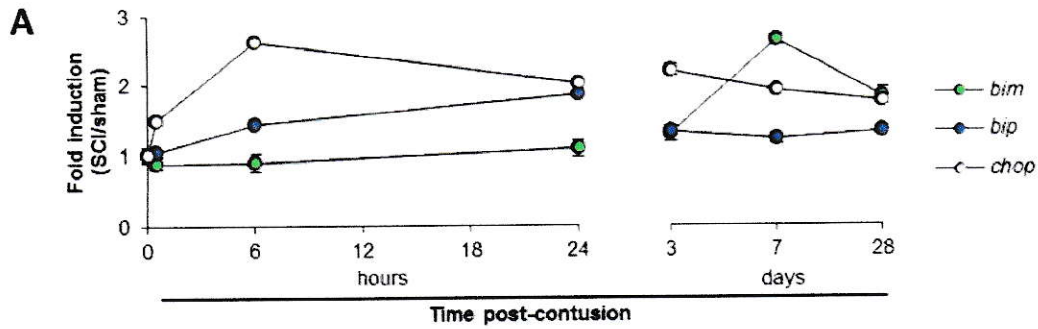


**Fig. S3. *Xbp1s* gene transfer with AAVs enhances locomotion recovery after SCI.** Wild type mice were hemisectioned at the T12 vertebral level and immediately injected into the injury site with 2  $\mu$ l ( $10^{12}$  DRP/mL) of AAV-GFP or AAV-Xbp1s/GFP. Locomotion recovery pattern was monitored before (0d) and after spinal cord hemisection and viral transduction with AAV-GFP or AAV Xbp1s/GFP using the Basso Mouse Scale (BMS) open field test. The BMS subscore, which assesses fine locomotor capabilities was scored and individual parameters of this subscore are presented at 28 and 35 days post surgery. Mean  $\pm$  SEM. \*,  $p < 0.05$ ; \*\*,  $p < 0.005$ .  $n = 8$  animals per group. Student's *t*-test.



**B**

Fold induction (SCI / sham)	Time post-surgery						
	hours				days		
	0	0.5	6	24	3	7	28
<i>edem</i>	1	0.84	0.88	1.22	1.87	1.62	1.32
<i>sec61</i>	1	0.92	0.99	2.14	1.57	2.13	1.53
<i>grp58</i>	1	0.78	0.92	1.23	2.10	2.81	1.29
<i>xbp-1</i>	1	1.05	1.13	1.50	1.16	1.04	1.34
<i>grp78</i>	1	1.06	1.47	1.90	1.36	1.24	1.36
<i>ho1</i>	1	1.08	2.38	5.68	3.23	1.93	1.39
<i>bim</i>	1	0.89	0.9	1.11	1.29	2.65	1.83
<i>atf4</i>	1	1.16	1.74	2.06	1.24	1.20	0.89
<i>chop</i>	1	1.49	2.64	2.03	2.21	1.95	1.75
<i>calnexin</i>	1	1.03	1.11	1.26	0.86	0.95	1.01
<i>calreticulin</i>	1	1.13	1.09	1.57	1.06	1.18	1.29
<i>actin</i>	1	0.97	0.96	1.16	0.93	0.85	1.18

**Fig. S4. Analysis of UPR markers from the microarray GDS2159 in the T8 spinal cord segment up to 28 days after moderate contusion injury. (A)** Expression levels of the indicated genes at different times after moderate spinal cord contusion in wild type mice obtained from the GDS2159 microarray data. Relative expression levels were normalized with actin mRNA levels and then sham normalized. **(B)** Table showing relative fold-induction values of UPR markers after moderate spinal cord contusion in wild type mice relative to control values (non-injured). Data was obtained from the microarray GDS2159 available at GEO dataset browser (<http://www.ncbi.nlm.nih.gov/sites/GDSbrowser?acc=GDS2159>).